Quadrupole Nutation NMR in Solids *

W. S. Veeman

Nijmegen SON Research Center for Molecular Structure, Design and Synthesis, University of Nijmegen, Nijmegen, The Netherlands

Z. Naturforsch. **47a**, 353–360 (1992); received July 18, 1991

The nutation frequency of a quadrupolar spin I depends on the quadrupole interaction. From nutation spectra, therefore, one obtains information about the direct surrounding of the atom. The theory of the straightforward and of more complicated nutation NMR experiments is outlined. Two applications of nutation NMR, to ^{23}Na in zeolites and ^{27}Al in alumina, are shown. In this way in $CaO \cdot 6\,Al_2O_3$ penta-coordinated aluminum has been detected.

I. Introduction

Nuclei with a nuclear spin quantum number I greater than 1/2 possess an electrical quadrupole moment that can interact with electric field gradients existing at the nucleus. This electric quadrupole interaction can provide valuable information about the local structure in solid materials where the electric field gradients arise from the charges surrounding the nucleus. The determination of the parameters describing the quadrupole interaction is traditionally the field of nuclear quadrupole resonance, NQR, and although NQR has many advantages, in many cases the one disadvantage is the low sensitivity of the experiment for nuclei with small quadrupole moments.

Several techniques have been invented in the past to circumvent this problem, especially by combination with the NMR experiment in a high magnetic field. A recent example of this combination is the zero-field NMR experiment where the evolution of the spins after excitation is studied with the sample outside the magnet while the signal is detected in the magnet [1].

In a normal NMR experiment of a quadrupole spin the price one pays for the relatively high sensitivity is a broadening of the NMR line due to the anisotropy of the quadrupole interaction of a spin in a magnetic field.

At this point we should distinguish the quadrupole line broadening of spins with integer spin quantum number I and half-integer I. When the quadrupole interaction is appreciably smaller than the interaction of the spin with the magnetic field (i.e. for strong fields or small quadrupole interactions), then for half-integer spins the $\Delta m = 1$ transition between the Zeeman states $m = 1/2$ and $m' = -1/2$ is broadened by second-order quadrupole interaction only [2], while in all other cases, for integer and half-integer spins, all $\Delta m = 1$ transitions are broadened in first order. In many practical cases this means that it is relatively easy to measure the $1/2 \leftrightarrow -1/2$ transition of half-integer spins, but that at the same time the determination of the quadrupole parameters from this broadened line is difficult or inaccurate due to the presence of other line broadening interactions. Some of these interactions may be eliminated by magic angle spinning, but the width of the quadrupole $1/2 \leftrightarrow -1/2$ powder spectrum is then also further reduced.

Here we want to discuss a technique, nutation NMR, proposed by Samoson and Lippmaa [3], where in a two-dimensional NMR fashion the effect of the quadrupole interaction is separated from other line broadening interactions, thereby increasing the information content of the spectra. The theory will be discussed for stationary samples, but later the effect of magic angle spinning will be considered.

II. Theory

The two-dimensional nutation NMR experiment is schematically indicated in Figure 1. During the evolution period t_1 in the two-dimensional NMR experiment the spins are subjected to a resonant rf field of strength $\omega_1 = \gamma B_1$ and phase x. During this pulse in a frame rotating around the static external field the

* Presented at the XIth International Symposium on Nuclear Quadrupole Resonance Spectroscopy, London, United Kingdom, July 15–19, 1991.

Reprint requests to Prof. W. S. Veeman, Physikalische Chemie, Universität-GH-Duisburg, Lotharstrasse 1, 4100 Duisburg, BRD.

0932-0784 / 92 / 0100-0353 $ 01.30/0. – Please order a reprint rather than making your own copy.

Dieses Werk wurde im Jahr 2013 vom Verlag Zeitschrift für Naturforschung in Zusammenarbeit mit der Max-Planck-Gesellschaft zur Förderung der Wissenschaften e.V. digitalisiert und unter folgender Lizenz veröffentlicht: Creative Commons Namensnennung-Keine Bearbeitung 3.0 Deutschland Lizenz.

This work has been digitalized and published in 2013 by Verlag Zeitschrift für Naturforschung in cooperation with the Max Planck Society for the Advancement of Science under a Creative Commons Attribution-NoDerivs 3.0 Germany License.

Zum 01.01.2015 ist eine Anpassung der Lizenzbedingungen (Entfall der Creative Commons Lizenzbedingung „Keine Bearbeitung") beabsichtigt, um eine Nachnutzung auch im Rahmen zukünftiger wissenschaftlicher Nutzungsformen zu ermöglichen.

On 01.01.2015 it is planned to change the License Conditions (the removal of the Creative Commons License condition "no derivative works"). This is to allow reuse in the area of future scientific usage.

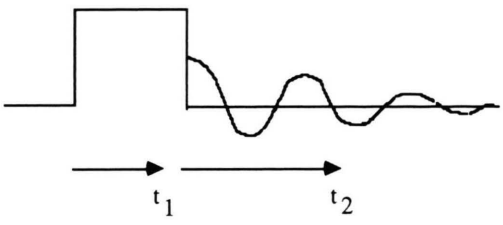

Fig. 1. Pulse scheme for nutation experiment; during t_1 a rf pulse is applied and during t_2 the FID detected. t_1 is stepwise incremented in steps of 1 or 2 μs to 64 or 128 μs.

Hamiltonian can be written as

$$H = \omega_1 I_x + \omega_q [3 I_z^2 - I(I+1)] \qquad (1)$$

with

$$\omega_q = \frac{e^2 q Q}{8 I(2I-1)} (3\cos^2\theta - 1 + \eta \cos 2\phi \sin^2\theta),$$

and where it is assumed that the quadrupole interaction, defined by the parameters $e^2 q Q$ and η, is much smaller than the interaction of the spins with the static external field. The angles θ and ϕ define the orientation of the quadrupole tensor relative to the external static magnetic field.

During the pulse the magnetization precesses around the x axis in the rotating frame with a frequency determined by the eigenvalues of the Hamiltonian (1). We know that for a spin I there are $2I+1$ eigenstates, and therefore in theory there could be $I(2I+1)$ different transitions and different nutation frequencies. Not all of these transitions are "allowed" and it can be derived [4] that for the nutation experiment described here, for a spin $I=3/2$ only four nutation frequencies are possible (see Fig. 2) between eigenstates with energies

$$E_1 = (1/2)\omega_1 + D_-, \qquad E_2 = (1/2)\omega_1 - D_-,$$
$$E_3 = (-1/2)\omega_1 + D_+, \qquad E_4 = (-1/2)\omega_1 - D_+,$$

where

$$D_\pm = (\omega_1^2 \pm \omega_1 \omega_q + \omega_q^2)^{1/2}.$$

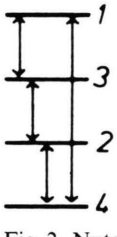

Fig. 2. Nutation transitions between rotating frame eigenstates for $I=3/2$.

These frequencies are functions of ω_1 and ω_q, and therefore of the orientation angles θ and ϕ. For a powder this results in a characteristic powder spectrum for each of the four nutation frequencies, see Figure 3. The total nutation spectrum is of course the sum of the four independent spectra. Fortunately, the nutation spectra are not always as complex as in Figure 3. Figure 4 shows calculated nutation spectra for a spin $I=3/2$ and $I=5/2$ as a function of the ratio ω_1/ω_q [5], and it is clear that only for intermediate ratios the nutation spectra are very complicated. The spectra are simple in the two extreme cases where either ω_1 is much smaller than ω_q or much larger. For small ω_q the nutation frequency is ω_1, for the other extreme case this frequency amounts to $(I+1)\omega_1$. Nutation NMR can therefore be used to estimate the quadrupole parameters.

In the 2D experiment of Fig. 1 the nutation spectrum can be measured by recording the free induction decay (FID) during t_2 for rf pulses with stepwise increasing length t_1. A two-dimensional Fourier transformation with respect to t_1 and t_2 then yields a two-dimensional NMR spectrum along two frequency axes F_1 and F_2. The projection along F_2 of the spectrum represents the normal spectrum with or without MAS, depending on how the experiment is performed. The spectrum along F_1 corresponds to the nutation spectrum. It may seem that several nutation spectra can be defined, depending on which transition in the

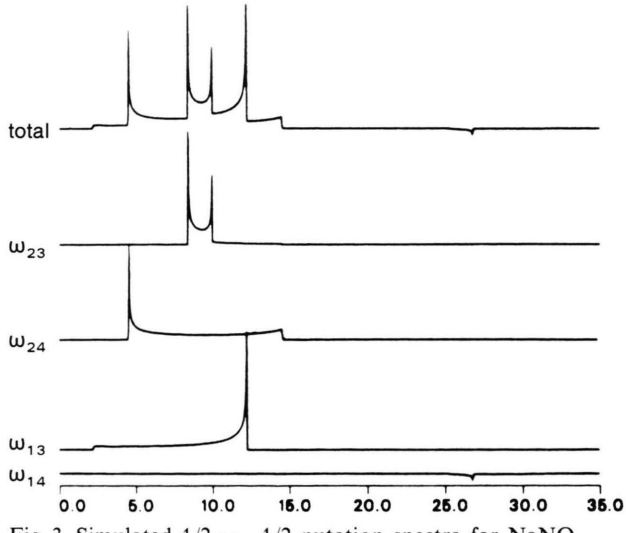

Fig. 3. Simulated $1/2 \leftrightarrow -1/2$ nutation spectra for $NaNO_3$ showing the separate powder lineshapes for each nutation transition of Figure 2.

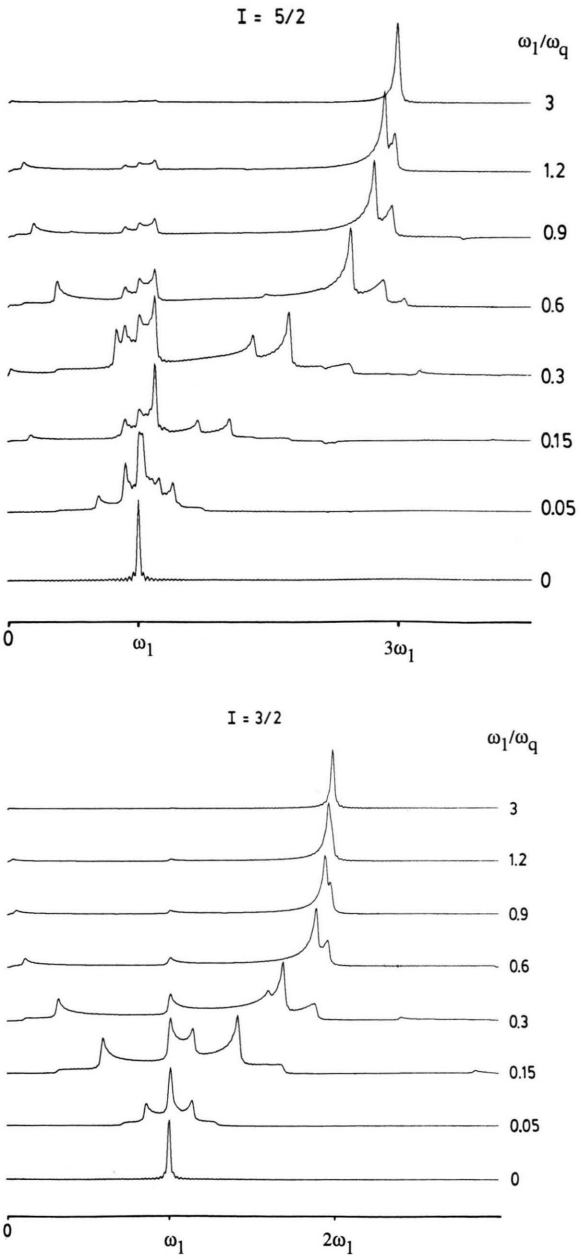

Fig. 4. Simulated nutation spectra for $I=3/2$ and $I=5/2$ for different ratios of ω_1/ω_q.

F_2 dimension ("laboratory frame transition") is detected, but fortunately this is not the case. Therefore in the following we will only consider nutation spectra detected via the $m=1/2 \leftrightarrow m=-1/2$ transition.

For the situation where there is both second-order quadrupole broadening of the $1/2 \leftrightarrow -1/2$ transition in the F_2 dimension and an intermediate ω_1/ω_q ratio, Fig. 5 shows a characteristic 2D nutation spectrum.

In most practical cases, however, the line shape is less characteristic.

Before considering more complex nutation experiments we want to show some applications to make clear what one can and cannot expect from nutation NMR.

III. Applications of Nutation NMR

Nutation NMR has been applied by several authors. Here we show two examples from our laboratory. Figure 6 shows the ^{23}Na ($I=3/2$) nutation spectra of the zeolite NaA as a function of hydration [6]. The complex pattern parallel to the F_2 axis in the spectrum of the dried sample is due to Na cations at three different sites in the zeolite (Fig. 7): in 6-rings, in 8-rings and in 4-rings. The 6-ring sodiums give rise to the two outer (i.e. along F_2) peaks (quadrupole "doublet") while the 8- and 4-ring ions cause the structured inner peak. Their position along the F_1 dimension at about $2\omega_1$ ($=(I+1)\omega_1$ for Na) indicates that all three Na types have a large quadrupole interaction, even though the 6-ring and 4-ring Na ions are located on a symmetry axis. On stepwise hydration until about 4 molecules H_2O per unit cell there is hardly a change in the spectra but starting from the fifth molecule H_2O the outer doublet due to the 6-ring ions starts to decrease until it is practically gone after the 15th molecule. Its intensity has shifted to a lower nutation frequency but the line in the F_1 dimension has broadened. With the addition of more water the line becomes very narrow in the F_2 dimension and in the F_1 dimension becomes more or less symmetrically centered around the nutation frequency ω_1. The picture that evolves is that the first four molecules of water are absorbed around the 8- and 4-ring Na ions, four ions in total, and have little effect on the local symmetry. From the 5th H_2O molecule on, the water is absorbed at sites where the local symmetry of the 6-ring Na ions is affected, making the symmetry high, corresponding to a small quadrupole interaction. With an excess of water all Na ions experience a high local symmetry. A surprising effect is the broadening in the F_1 direction upon hydration, we shall discuss this later. Note that these spectra are taken without magic angle spinning.

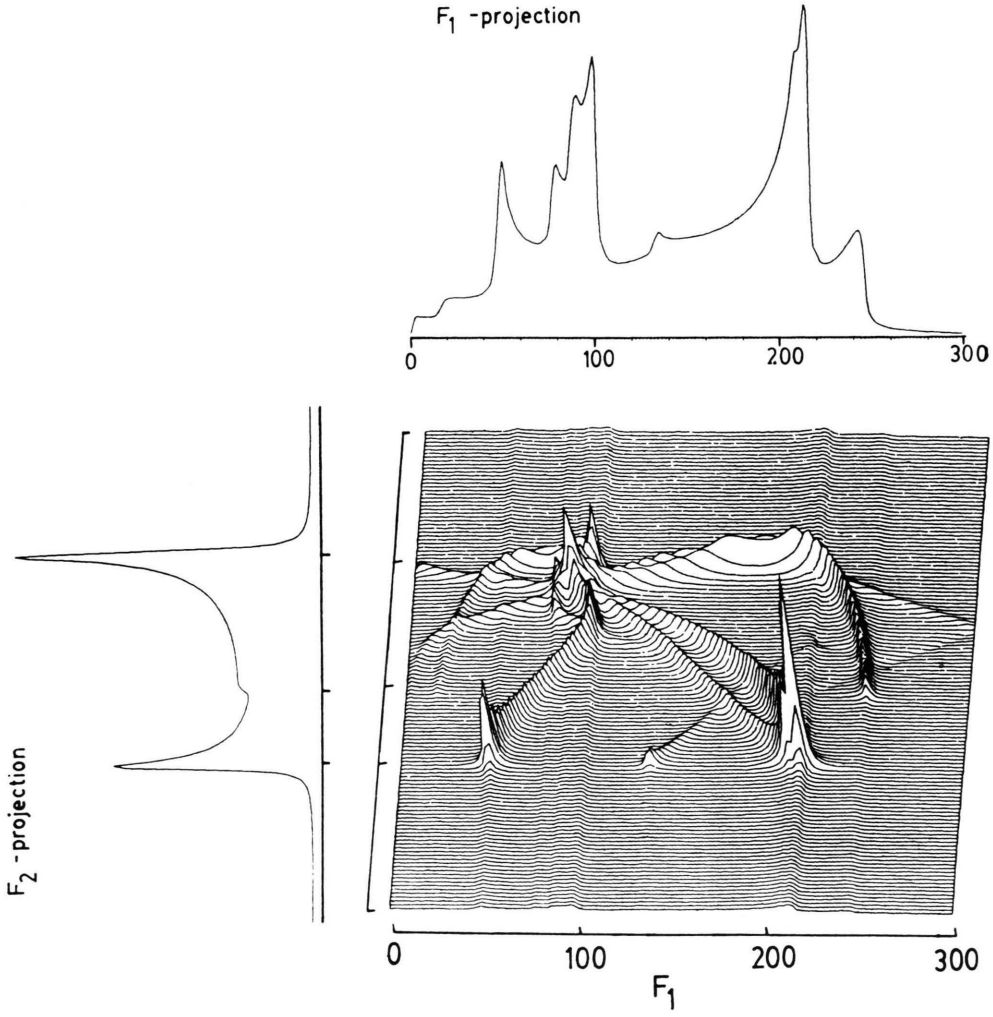

Fig. 5. Simulated 2D nutation spectrum for $I=5/2$ with $\omega_1/\omega_q=0.45$ and $\eta=0$.

Another application of nutation NMR was prompted by the thesis of van Hoek [7] who investigated the structure of $CaO \cdot 6Al_2O_3$ by NMR. From his results he concluded that no penta-coordinated aluminum could be detected because of too much second-order quadrupole broadening. Müller and coworkers [8] reached the same conclusion. Figure 8a shows van Hoek's 156 MHz ^{27}Al MAS NMR spectrum, reproduced by Ruinaard [9]. Van Hoek assigned the signals at 9 and 16 ppm to octahedrally coordinated aluminum and the signal(s) at 66 ppm to tetrahedrally coordinated aluminum. Careful examination of this spectrum, however, reveals a broad line under the 16 ppm peak, as is especially clear from the line-narrowed spectrum in Figure 8b. From the corresponding nutation spectrum two cross-sections parallel to F_2, at ω_1 and $3\omega_1$, are shown in Figure 9. The strong broad line at around 16 ppm is absent in the ω_1 section but present in the $3\omega_1$ section. This proofs that the spins responsible for the broad line experience a quadrupole interaction larger than that of the tetra- and octahedrally coordinated aluminums.

The ^{27}Al quadrupole coupling constant e^2qQ in a simple point charge model is given by [10]

$$e^2qQ = (1-\gamma_\infty)\frac{e^2qQ}{4\pi\varepsilon_0 h}\sum_i \frac{q_i(3\cos^2\theta_i - 1)}{r_i^3},$$

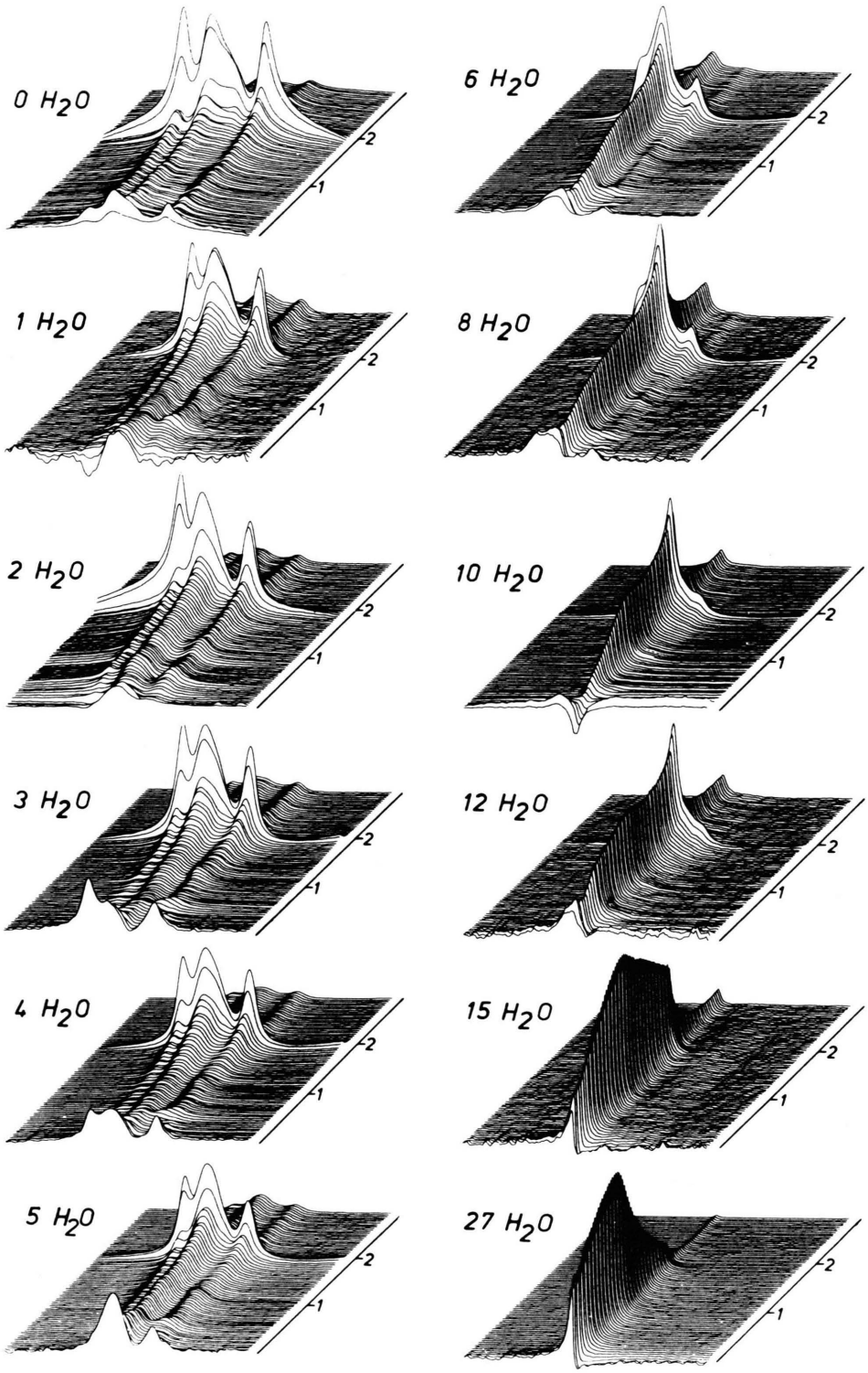

Fig. 6. ^{23}Na nutation spectra of zeolite NaA as functions of hydration. The horizontal axis is the F_2 axis and the numbers along F_1 indicate $1\omega_1$ and $2\omega_1$.

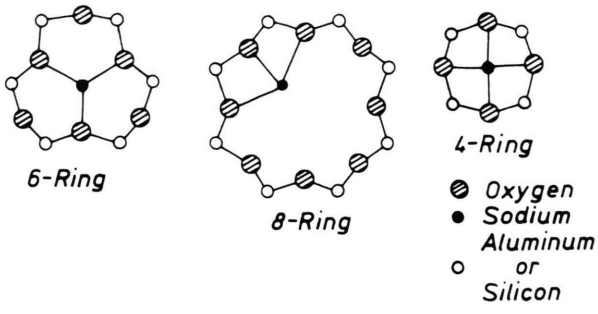

Fig. 7. The 12 sodium sites in NaA, 8 in rings with 6 oxygens, 3 in rings with 8 oxygens and 1 in a ring with 4 oxygens.

where

γ_∞ = Sternheimer factor = -2.298,

Q = ^{27}Al quadrupole moment = 0.15×10^{-28} m^2,

eq_i = charge at distance r_i from aluminum.

In the bipyramid configuration of Fig. 10 θ_i is the angle between r_i and the pyramid axis. With $R=$ 2.189 Å, $r=1.734$ Å and $q_i=-2$ (pure ionic bonds) we find

$$e^2qQ = -2(1-\gamma_\infty)\frac{e^2qQ}{4\pi\varepsilon_0 h}\left\{\frac{4}{R^3}-\frac{3}{r^3}\right\} = 6.6 \text{ MHz}.$$

Clearly the symmetry dictates that $\eta=0$.

From the nutation experiment and van Hoek's experiments at lower magnetic field we can estimate the quadrupole parameters of the spin species responsible for the broad line discussed above: $e^2qQ=6.7$ MHz, $\eta=0$ and an isotropic chemical shift of 27.5 ppm [9]. This agrees well with the simple bipyramid model discussed above, so we assume that the broad NMR line in Fig. 8 at around 16 ppm is due to penta-coordinated aluminum. The simple point charge calculation also seems to indicate that the split atom model of the bipyramid aluminum, where the aluminum jumps between two sites, symmetrically on the pyramid axis, as proposed by Utsunomiya et al. [11], is not realistic since it can easily be seen from the calculation above and from Fig. 10 that for such a case the quadrupole interaction quickly decreases and will become much smaller than the experimental value. The nutation spectra, of which we show here cross-sections, have been made with magic angle spinning. It is not difficult to see that when the magic angle spinning frequency is relatively low so that during the nutation pulses the orientation of the spinner does not appreciably change, the effect of magic angle spinning on the nutation spectra can be neglected.

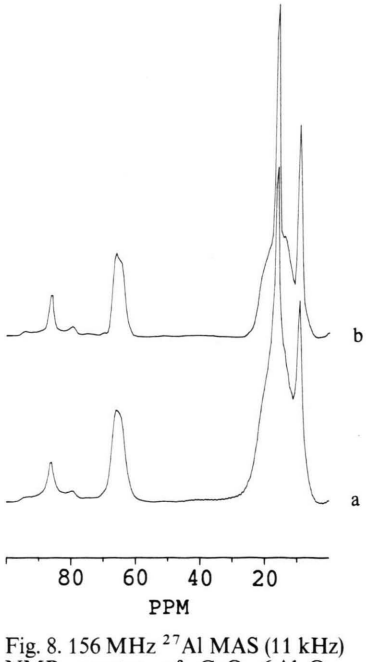

Fig. 8. 156 MHz ^{27}Al MAS (11 kHz) NMR spectra of $CaO \cdot 6Al_2O_3$, (a) without and (b) with line narrowing.

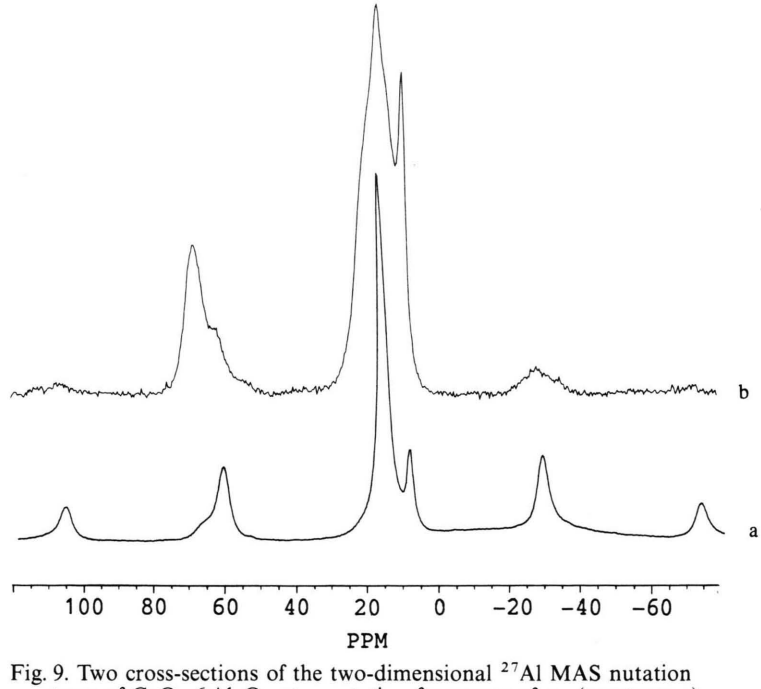

Fig. 9. Two cross-sections of the two-dimensional ^{27}Al MAS nutation spectrum of $CaO \cdot 6Al_2O_3$ at a nutation frequency of ω_1 (spectrum a) and $3\omega_1$ (spectrum b).

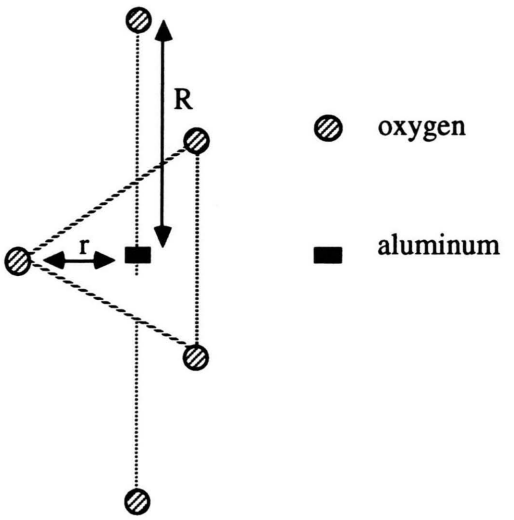

Fig. 10. The bipyramidal configuration of penta-coordinated aluminum in $CaO \cdot 6\,Al_2O_3$; the distances R and r are given in the text.

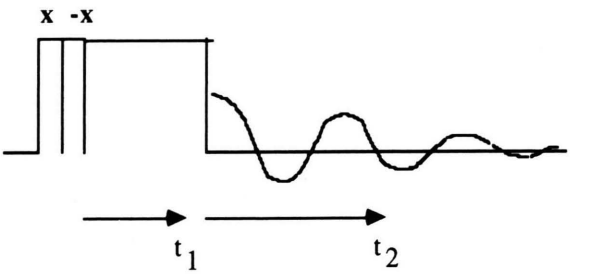

Fig. 11. The nutation experiment preceded with two pulses of opposite phase and fixed length, the rotary echo nutation experiment.

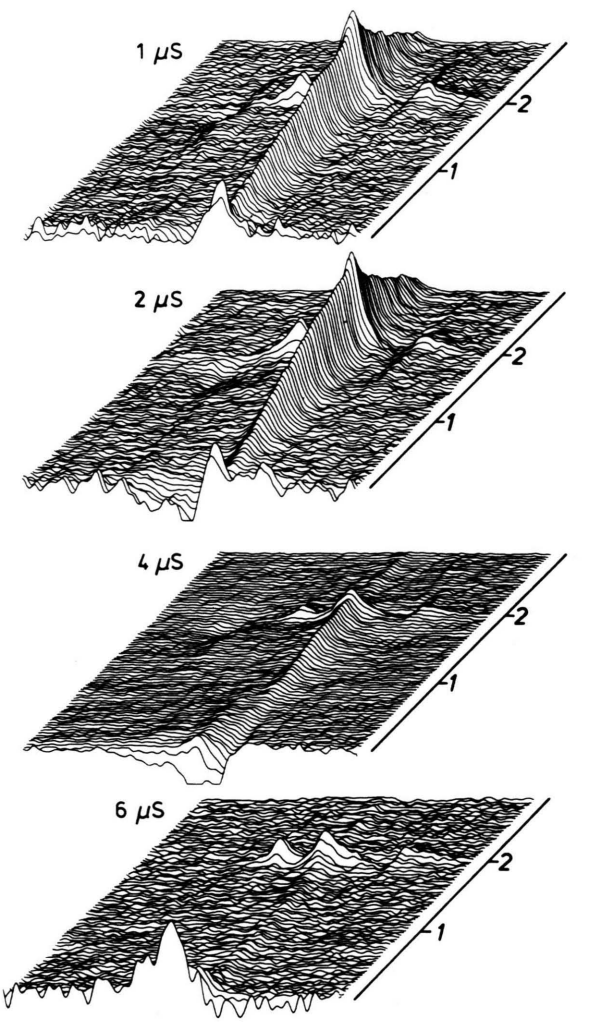

Fig. 12. The ^{23}Na rotary echo nutation spectra of partly hydrated (6 molecules H_2O per unit cell, see also Fig. 6) NaA. The length of the rotary echo pulses are increased from 1 μs to 6 μs.

IV. More Nutation NMR

An extension of the nutation NMR experiment of Fig. 1, the rotary echo experiment, is suggested by the results on NaA as discussed above. Clearly the spectra of the hydrated zeolite do not resemble the simulated spectra of Fig. 4, the linewidth is much broader. This is a relaxation effect as the following experiment (Fig. 11) shows [12]. Here the nutation pulse is preceded by two short pulses with opposite phase, say x and $-x$. For NaA with 6 H_2O molecules per unit cell a pulse length of only 6 μs is enough to suppress the broad nutation line (Figure 12). Clearly the width of nutation lines can be affected by short $T_{2\varrho}$ values when fluctuations are present with a frequency component of the order of the splittings between the eigenstates of the rotating frame Hamiltonian (1), of the order of 100 kHz [12].

The nutation experiment of Fig. 1 is conceptually the most simple one. However, as we have seen in Figs. 3 and 4, the nutation spectra are not in general simple. The reason is that there are many different nutation frequencies and that each nutation frequency gives rise to a powder spectrum. We have also remarked that not all transitions between the rotating frame eigenstates correspond to a nutation frequency. For instance of the 6 possible nutation frequencies of a spin $I = 3/2$ two are missing, see Figure 2. The nutation experiment could become more valuable when

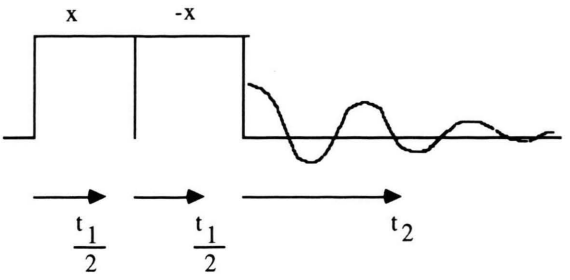

Fig. 13. The x, $-x$ nutation experiment; the length of both pulses is stepped.

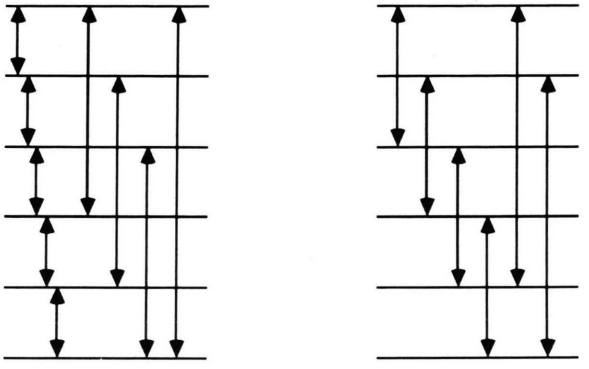

x nutation x,-x nutation

Fig. 14. A comparison between the allowed nutation frequencies in the x and x, $-x$ nutation experiment.

the pulse sequence would select out only one nutation frequency. In the $x\,\bar{x}$ nutation experiment the nutation rf pulse is split into two pulses with opposite phase (Figure 13). Analysis [4] shows that the $x\,\bar{x}$ experiment for a spin $I=3/2$ again has four nutation frequencies, the two frequencies that are missing in the x nutation experiment plus the sum and difference of these two frequencies. Although we can hardly say for this approach that the spectrum has been simplified with respect to the x experiment, it does show that it may be worthwhile to investigate the result of composite nutation pulses. Figure 14 shows schematically the nutation frequencies of the x and $x\,\bar{x}$ nutation experiment for $I=5/2$. Again the x nutation experiments give the odd "multiple quantum" nutation frequencies and the $x\,\bar{x}$ experiment the even "multiple quantum" frequencies.

V. Conclusions

Nutation NMR is a helpful technique to unravel in spectra of quadrupolar nuclei the contribution of the quadrupole interaction to the total shift from the chemical shift. The information one obtains about the quadrupole parameters in most cases is rather qualitative, the technique is most useful when nuclei with clearly different quadrupole interactions have to be distinguished. The main difficulty in the interpretation is the complex spectrum that results from a nutation experiment since it can consist of many overlapping powder patterns.

[1] D. B. Zax, A. Bielecki, K. W. Zilm, A. Pines, and D. P. Weitekamp, J. Chem. Phys. **83,** 4877 (1985).
[2] A. Abragam, The principles of nuclear magnetism, Clarendon Press, Oxford 1961.
[3] A. Samoson and E. Lippmaa, Chem. Phys. Letters **100,** 205 (1983).
[4] R. Janssen and W. S. Veeman, J. Chem. Soc., Faraday Trans. 1, **84,** 3747 (1988).
[5] A. P. M. Kentgens, J. J. M. Lemmens, F. M. M. Geurts, and W. S. Veeman, J. Magnetic Resonance **71,** 62 (1987).
[6] G. A. H. Tijink, R. Janssen, and W. S. Veeman, J. Amer. Chem. Soc. **109,** 7301 (1987).
[7] J. van Hoek, Thesis, Technical University Eindhoven, The Netherlands 1990.
[8] D. Müller, W. Gessner, A. Samoson, E. Lippmaa, and G. Scheler, Polyhedron **5,** 779 (1986).
[9] R. Ruinaard, A. P. M. Kentgens, and W. S. Veeman, to be published.
[10] C. P. Slichter, Principles of Magnetic Resonance, Springer Verlag, Berlin, 1989.
[11] A. Utsunomiya, K. Tanaka, H. Morikawa, and F. Marumo, J. Solid State Chem. **75,** 197 (1988).
[12] R. Janssen, G. A. H. Tijink, and W. S. Veeman, J. Chem. Phys. **88,** 518 (1988).